Monthly Notices
of the
ROYAL ASTRONOMICAL SOCIETY

MNRAS **492,** L22–L27 (2020)
Advance Access publication 2019 November 28

doi:10.1093/mnrasl/slz176

Measurement of the spin of the M87 black hole from its observed twisted light

Fabrizio Tamburini [1]★ Bo Thidé [2]★ and Massimo Della Valle [3,4]★

[1] *ZKM, Lorenzstraße 19, Karlsruhe D-76135, Germany*
[2] *Swedish Institute of Space Physics, Ångström Laboratory, Box 537, SE-751 21 Uppsala, Sweden*
[3] *Capodimonte Astronomical Observatory, INAF-Napoli, Salita Moiariello 16, I-80131 Naples, Italy*
[4] *European Southern Observatory, Karl-Schwarzschild-Straße 2, D-85748 Garching bei München, Germany*

Accepted 2019 November 25. Received 2019 November 25; in original form 2019 July 2

ABSTRACT

We present the first observational evidence that light propagating near a rotating black hole is twisted in phase and carries orbital angular momentum (OAM). This physical observable allows a direct measurement of the rotation of the black hole. We extracted the OAM spectra from the radio intensity data collected by the Event Horizon Telescope from around the black hole M87* by using wavefront reconstruction and phase recovery techniques and from the visibility amplitude and phase maps. This method is robust and complementary to black hole shadow circularity analyses. It shows that the M87* rotates clockwise with an estimated rotation parameter $a = 0.90 \pm 0.05$ with an ~ 95 per cent confidence level (c.l.) and an inclination $i = 17^\circ \pm 2^\circ$, equivalent to a magnetic arrested disc with an inclination $i = 163^\circ \pm 2^\circ$. From our analysis, we conclude that, within a 6σ c.l., the M87* is rotating.

Key words: black hole physics – gravitational lensing: strong – methods: data analysis – methods: numerical – techniques: image processing.

1 INTRODUCTION

Most of the knowledge we have about the Universe comes from observing and interpreting its electromagnetic (EM) radiation. This ranges from visible light caught by the naked eye, to radio and higher photon energy emissions intercepted by advanced telescopes. The information carried by the EM field is encoded, naturally or artificially, into conserved quantities (observables) of the field that are transported from the source to the distant observer where the information can be decoded and recovered. The standard observables are the well-known 10 conserved quantities that are concomitant with the ten-dimensional Poincaré group of Noether invariants: the field energy (a single scalar), used, e.g. in radiometry, linear momentum (three components of a vector), used in, e.g. radio communications, angular momentum (three components of a pseudo-vector), used only partially in radio science and technology, and the centre of energy (three components of a vector).

Of these observables, we used, for the first time, the EM angular momentum, which is related to rotation and torque action (Torres & Torner 2011), to measure the rotation of the M87* black hole in a novel way. This observable has not yet been fully exploited in astronomy (Harwit 2003; Anzolin et al. 2008; Thidé et al. 2011). The total angular momentum $\boldsymbol{J}$ comprises two, in general inseparable, quantities: (1) the spin angular momentum $\boldsymbol{S}$ (SAM), associated with photon helicity, i.e. the wave polarization, and (2) the orbital angular momentum (OAM) $\boldsymbol{L}$, associated with the torque action and EM vorticity. EM waves carrying OAM are also known as 'twisted waves'. This property remains valid down to the single photon level as superpositions of photon eigenstates, each with a well-defined value of SAM and OAM, as described in Molina-Terriza, Torres & Torner (2007). Only in the paraxial approximation, $\boldsymbol{S}$ and $\boldsymbol{L}$ behave as two separate variables. OAM-carrying beams permit the encoding and extraction of more information into and from the EM radiation emitted by a distant source than any existing method that is based on the intensity of the field only (Torres & Torner 2011; Tamburini et al. 2012). In 2011, a theoretical–numerical study published by Tamburini et al. (2011a) showed that light and radio emitted from an accretion disc (AD) around a massive rotating black hole are expected to be endowed with specific distributions of OAM due to the model of the AD and general relativity (GR) effects such as Kerr space–time dragging and mixing and gravitational lensing. An example is the Einstein ring, such as that in the M87 galaxy as observed by the EHT team, which surrounds the black hole. The Einstein ring is created by gravitationally lensed beams that, experiencing an anamorphic transformation (Beckwith & Done 2005), is also accompanied by a polarization rotation (Su & Mallett 1980) due to the gravitational Faraday effect (Dehnen 1973), image deformation, and rotation due to the lensing of the curved space–time as well as other modifications in the phase wavefront, including

★ E-mail: fabrizio.tamburini@gmail.com (FT), bt@irfu.se (BT), massimo.dellavalle@inaf.it (MDV)

gravitational Berry phase effects (Carini et al. 1992; Feng & Lee 2001; Yang & Casals 2014).

Light propagating near rotating black holes experiences a behaviour that is analogous to that experienced in an inhomogeneous anisotropic medium in a mechanism related to the Pancharatnam–Berry geometric phase (De Zela 2012). This involves spatially inhomogeneous transformations of the polarization vector in the observation plane of an asymptotic observer causing the lensed light to acquire OAM. The OAM present in that light can be univocally characterized by the so-called spiral spectrum (Torner, Torres & Carrasco 2005), to be discussed more in detail in the 'Methods' section, revealing the rotation of the Black Hole (BH). Because of the properties of the Kerr metric, the OAM content in the EM radiation lensed by the Kerr black hole (KBH) and the associated spatial distribution of the azimuthal phase $\phi(\varphi)$ depend only on the observable inclination i of the KBH equatorial plane with respect to the observer and the rotation parameter $a = J_{\rm BH}/(m_{\rm BH}c)$, where $J_{\rm BH}$ is the KBH angular momentum, but not on the mass $m_{\rm BH}$ of the BH (Tamburini et al. 2011a).

Here we report the first observational confirmation of such GR-induced OAM vorticity, detected in the public brightness temperature data (EHT Collaboration 2019a) and also from the visibility amplitude and phase maps from the Event Horizon Telescope (EHT) observations at $\lambda = 1.3$ mm of the central compact radio source surrounding a supermassive black hole M87* in the galaxy M87 of the Virgo Cluster released by the EHT team (EHT Collaboration 2019b,c,d,e,f,g). Exploiting this OAM, we were able to directly measure the spin, sense of rotation, and inclination of M87*.

2 METHODS

The key tool to determine the BH rotation parameter a is the so-called spiral spectrum. Torner et al. (2005) ideated this method that uniquely identifies the OAM content in the EM radiation, using the fundamental physical property that any light beam can be decomposed into a set of discrete orthogonal eigenmodes, each carrying its own well-defined OAM quantity and known geometry. A convenient choice is Laguerre–Gaussian modes. In cylindrical polar coordinates (ρ, φ, z), these paraxially approximate modes describe an EM field at z with an amplitude (Barnett & Allen 1994)

$$u_{m,p}(r,\theta,z) = \sqrt{\frac{2p!}{\pi(p+m)!}}\frac{1}{w(z)}\left[\frac{r\sqrt{2}}{w(z)}\right]^{l} L_p^m\left[\frac{2r^2}{w^2(z)}\right] \times \exp\left[\frac{-ikr^2}{2R(z)} - \frac{r^2}{w(z)^2}\right] \times \exp\left[-i(2p+m+1)\arctan\left(\frac{z}{z_{\rm R}}\right)\right] e^{-im\varphi}, \quad (1)$$

where m is the azimuthal index that describes the z component of OAM, i.e. the number of twists in the helical wavefront (the topological charge), p is the radial node number of the mode, $z_{\rm R}$ is the Rayleigh range of the beam, $w(z)$ is the beam waist, $R(z)$ is the radius of curvature, L_p^m is the associated Laguerre orthogonal polynomial, and φ is the azimuthal phase of the beam. The decomposition of a beam into orthogonal modes will give the spectrum of OAM states carried by the EM wavefront, i.e. the spiral spectrum.

Thus, to estimate the rotation of M87*, this is, step by step, the procedure that we followed:

(i) Using the KERTAP software (Chen et al. 2015), we simulated numerically different scenarios of an Einstein ring by varying the emission parameters of the AD, the inclination of the BH spin i, and the BH rotation parameter a of a KBH. For each simulation, we obtained, in the image plane of an asymptotic observer, the field intensity, polarization, and phase distributions, and determined the content of OAM from the spiral spectrum (Torner et al. 2005), relating the physical properties of the BH system to that of the OAM distribution (Tamburini et al. 2011a) with the asymmetry parameter q. This quantity is the ratio of the height of the $m = 1$ component with respect to the $m = -1$ one found in each spiral spectrum. If $q > 1$, then the rotation is clockwise, while $q = 1$ indicates no rotation and $q < 1$ counterclockwise. This identifies the content of OAM in the field. From the results of the numerical simulations, from each AD model chosen in the simulations, we relate q with a fixed i by using polynomial interpolations.

(ii) From the EHT data, we extract the intensity I and reconstruct numerically the spatial phase distribution P of the field in the image plane of an asymptotic observer by using well-known phase reconstruction techniques based on the Transport of Intensity Equation (TIE; Barbero 2006; Schulze et al. 2012; Lubk et al. 2013; Kelly 2018; Ruelas, Lopez-Aguayo & Gutiérrez-Vega 2018) and build the spiral spectra.

(iii) We estimate the rotation parameter a from the comparison of the spiral spectrum of each numerical simulation with those obtained from the EHT data by using the asymmetry parameter q (Torres & Torner 2011).

We can use this technique with OAM states to determine the rotation parameter a building up the spiral spectrum for the M87* Einstein ring because the radio source has been spatially resolved at a 1.3 mm wavelength by the $\sim 10\,000$ km EHT radio-interferometric baseline. In this case, the wavefront is obviously not plane such as that emitted from a point-like source at infinity, even if the distance from the source to the Earth is $D = 54.8 \pm 2.6 \times 10^6$ light years ($D \sim 16.8$ Mpc). Hence, we can determine, within a good approximation, the OAM content in the wavefront from the OAM spectrum of the received radio waves. Furthermore, from the asymmetry parameter q of the observed OAM spectrum, we can determine the sense and magnitude of the rotation of the M87* and its inclination, verifying the theoretical predictions made by Tamburini et al. (2011a).

As seen from equation (1), this spectrum of OAM states carried by the EM wavefront is obtained by Fourier transforming the EM field with respect to the azimuthal angle φ. Since our twisted-light/OAM method operates in angular momentum space and uses the additional information encoded in the phase of the OAM beam, it is complementary to methods based on analyses in configuration (φ) space, such as the analysis of the deviation from the circularity of the M87* shadow adopted by the EHT team (Bambi et al. 2019; EHT Collaboration 2019b,c,d,e,f,g), a method that has so far not been able to yield any conclusive results. In fact, the geometry of the shadow in Kerr metric (Kerr 1963) and the radius of the photon ring (the photon-capture radius) change with the ray orientation relative to the angular momentum vectors with respect to that of a Schwarzschild BH. This results in a deformation of the circular shape of the black hole's shadow that was not possible to be determined with the available data. This deformation, even if small (< 4 per cent), will be potentially detectable only with future EHT acquisitions (EHT Collaboration 2019b); the data released so far only allow the EHT team to determine the inclination of the BH spin and the presence of a clockwise rotation, through the comparison of the experimental

data with about 60 000 templates of the Einstein ring and BH shadow obtained from numerical simulations.

Moreover, our method makes use of the additional information encoded in the phase of the OAM beam characterized by the asymmetry parameter q of the spiral spectrum due to the vorticity induced by the Kerr metric and emitted by a slightly larger region of the Einstein ring surrounding the BH, as explained more in detail in Tamburini et al. (2011a) and in the Supplementary Material (SM). Let us follow our procedure.

(i) Numerical simulations of OAM from the Einstein ring of a KBH. As initial step in the analysis and interpretation of the EHT data, we build up, with the help of the freely available software package KERTAP (Chen et al. 2015), a set of numerical simulations describing several scenarios of black hole ADs, as measured by an ideal asymptotic observer, to compare with the results of the analysis of the experimental data. The value of the rotation parameter varied in the interval $0.5 < a < 0.99$ clockwise and counterclockwise and the inclination $1^\circ < i < 179^\circ$. For the AD of the Einstein ring, we adopted a thermalized emission with $0.1 < \Gamma < 2$ power spectra, chosen in agreement with the ALMA observations (Doi et al. 2013; EHT Collaboration 2019f) and a radial power-law index that specifies the radial steepness of the profile, of $n_r = 3$; we also simulated synchrotron emission, Compton scattering, and bremsstrahlung. Regarding the AD model used to fit with the observations, as discussed by the EHT team in EHT Collaboration (2019g), we also find that, in any case, the image properties are determined mainly by the space–time geometry. KERTAP provides a detailed description of the propagation of light in Kerr space–time (Kerr 1963) with an error $\sim 10^{-7}$, in geometric units ($G = c = 1$) and OAM routines $\sim 10^{-12}$.

The OAM content is then numerically calculated from KERTAP output images and the Stokes polarization parameters (U, Q, V), analysing the parallel transport of the electric field and the Pancharatnam–Berry geometrical phase with the vectorial field technique developed by Zhang et al. (2015) where the radiation emitted from the simulated Einstein ring is a fully polarized vectorial vortex beam propagating in free space in the z-direction from the BH to the asymptotic observer. The resulting spatial distribution of the azimuthal phase $\phi(\varphi)$ of the radiation used to calculate the OAM and the associated OAM spiral spectrum are invariant with respect to the mass m_{BH} of the KBH and depend only on the parameters i and a (Tamburini et al. 2011a).

(ii) Analysis of the EHT data with OAM techniques. In order to construct the spiral spectrum (Torner et al. 2005), it is necessary to analyse, at each point in the image plane, the intensity (amplitude) and the phase and then calculate numerically the OAM content by interpolating the field with the different OAM modes described in equation (1). OAM beams are detectable and can be accurately characterized with interferometric techniques that directly measure amplitude, intensity, and phase, as has been demonstrated experimentally in the radio domain (Thidé et al. 2007; Tamburini et al. 2011b, 2012).

Since these kinds of data are not all available from the EHT observations, in order to obtain the spatial phase distribution, we had to reconstruct the evolution of the wavefront with the well-known non-interferometric technique based on the TIE method and reduced error procedure (Barbero 2006; Schulze et al. 2012; Lubk et al. 2013; Kelly 2018; Ruelas et al. 2018). The TIE equations (see equation 6 in SM par. 1.2) recover the phase evolution between two or more consecutive intensity images of a stable source, in the paraxial approximation, when the source itself is spatially translated

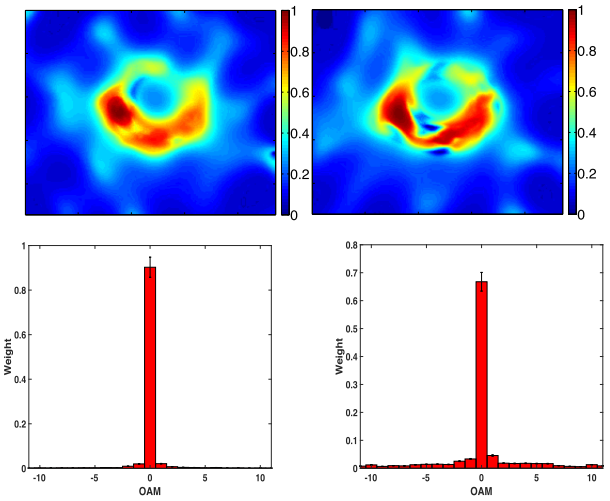

Figure 1. Experimental results. Normalized electric field component magnitudes along the observer's direction reconstructed from the TIE analysis of the brightness temperature in a finite-frequency bandwidth and for the corresponding spiral spectra for epoch 1 and epoch 2. The asymmetry q between the $m = 1$ and -1 components in both of the spiral spectra reveals the presence of twisted EM waves from the black hole Einstein ring (Tamburini et al. 2011a) with $a = 0.904 \pm 0.046$ rotating clockwise. The spin is pointing away from the Earth with an inclination between the approaching jet and the line of sight of $i = 17^\circ$ if the angular momentum of the accretion flow and that of the black hole are anti-aligned (equivalent to a similar geometry with an inclination $i = 163^\circ$, but where the angular momentum of the accretion flow and that of the BH are aligned). The Einstein ring has a gravitational radius $r = 5R_g$, as indicated by an EHT analysis dominated by incoherent emission (see EHT Collaboration 2019a, g, and the text). The image coordinates are in arbitrary units. The intensity sidebars are normalized to unity.

along the z-axis with respect to the observer. This is exactly what happens when the images of M87* were taken, because of its relative motion with respect to the Earth (for more details, see SM).

The two intensity and phase wavefront plots (see Fig. 1 in the main text and figs 1 and 2 in SM) have been reconstructed from two sets of two consecutive images of the Einstein ring of M87*. The two different observational runs of EHT are each separated by 1 d, the first being epoch 1 (2017 April 5 and 6), and the second being epoch 2 (2017 April 10 and 11). The data were obtained from 10 s of signal averaging as described in EHT Collaboration (2019a, e, f, g). The M87* exhibited a modest source evolution between the two pairs of nights April 5–6 and April 10–11 and a broad consistency within each pair.

Moreover, the TIE method can be applied because the physical evolution of the M87* Einstein ring structure during the two different EHT observation runs, each separated by 1 d, in two 2 GHz frequency bands centred on 227.1 and 229.1 GHz is negligible, and the source can be considered stable as already stated in EHT Collaboration (2019f) and Doeleman et al. (2012). More precisely, the evolution of the source during the time interval between the two sets of pairs of days was < 5 per cent within an observation (EHT Collaboration 2019d,e). Relative to the object, each day is $2.8R_g c^{-1}$ long for a BH with a mass $M = 6.5 \pm 0.2|_{stat} \pm 0.7|_{sys} \times 10^9$ $M_\odot$. This time-scale is shorter than the crossing time of light of the source plasma and short compared to the decorrelation time-scale of EHT simulations used to analyse the experimental results, $50R_g c^{-1}$ (EHT Collaboration 2019f). Only a small evolution was

Table 1. Table of values of the asymmetry parameter q, obtained by dividing the height of the $m = 1$ by that of $m = -1$ components of the spiral spectra (see the text and SM) of the light emitted in the neighbourhoods of a KBH with different rotation parameters $0.5 < a < 0.9$, versus the rotation parameter a for two sample inclinations $i = 17^\circ$ and 46°, simulated with KERTAP. The rotation is clockwise and averaged over different AD emission mechanisms characterized by $0.1 < \Gamma < 2$ power spectra. The error is $\sim 10^{-7}$. In agreement with EHT, we choose $i = 17^\circ$ (and $i = 163^\circ$).

BH rotation parameter a	0.50	0.60	0.80	0.90
Asymmetry parameter q	–	–	–	–
$i = 17^\circ$	1.295	1.320	1.356	1.391
$i = 46^\circ$	1.392	1.412	1.424	1.438

observed, with a maximum of a few per cent of difference between the two epochs, separated by 5 d (EHT Collaboration 2019a,g).

With the TIE method, one can estimate the OAM content from the brightness temperature distributions reported in the images (Rybicki & Lightman 2004) and then the rotation parameter of the KBH as it was obtained from two different and independent acquisitions. The TIE method remains valid even though the shift s along z due to the motion of our planet around the Sun in the interval of 1 d appears to be enormous with respect to the wavelength because the phase profile of an OAM wave repeats in space with a recurrence modulo λ. This bacause the OAM properties of the waves are not affected when they propagate in free space and cannot be affected after having propagated across the distance s, which is only a small fraction of the distance from M87* to the Earth.

The correctness of our procedure that uses the relative translational motion of the Earth with respect to M87* is mathematically ensured by the Wold theorem (Wold 1954; Anderson 1994), as explained in the SM.

(iii) Estimating the BH rotation parameter. The rotation parameter a can be estimated by comparing the asymmetry parameter q, given by the ratio of the OAM spectrum components $m = 1$ and -1, for any value of the inclination parameter $1^\circ < i < 179^\circ$ with a step of 1° obtained from the numerical simulations and the values of q obtained from the analysis of the EHT data of epochs 1 and 2. Table 1 shows an example of values of the parameter q obtained from the numerical simulations of the Einstein ring of a KBH for two values of the inclination parameter, $i = 17^\circ$, as indicated by EHT, and $i = 46^\circ$, obtained by varying the rotation parameter a. The variation of $i = 1^\circ$ can be adopted as indetermination in i as it induces a small change $\Delta q = 0.0012$ corresponding to $\Delta a \simeq 0.06$ compatible with the variation of a in its error interval. The spiral spectra reported in Fig. 1, obtained with the TIE imaging techniques, reveal the presence of an asymmetric ring with a clockwise rotation and a 'crescent' geometric structure that exhibits a clear central brightness depression. This indicates a source dominated by lensed emission surrounding the black hole shadow.

From the analysis of the two data sets, we obtain the asymmetry parameters $q_1 = 1.417 \pm 0.049$ for epoch 1 and $q_2 = 1.369 \pm 0.047$ for epoch 2. They yield an averaged asymmetry in the spiral spectrum of $\overline{q} = 1.393 \pm 0.024$ corresponding to $a = 0.904 \pm 0.046$ (see SM). The average value of the asymmetry parameter is compatible with that resulting from our numerical simulations, $q_{\rm numerical} = 1.389$, for an Einstein ring with a radius of 5 gravitational radii, emitting partially incoherent light around a KBH.

The values of q indicate that the KBH can have an inclination of $i = 17^\circ \pm 2^\circ$, with the angular momenta of the accretion flow and of the black hole anti-aligned, showing a clockwise rotation as described in EHT Collaboration (2019f), where an error of 1° was reported. The preferred inclination mentioned above is alternatively equivalent to a magnetically arrested disc scenario with an inclination $i = 163^\circ \pm 2^\circ$, and the angular momentum of the AD flow instead aligns with that of the black hole (Sob'yanin 2018). This is in agreement with the results of the EHT collaboration, presented and discussed in EHT Collaboration (2019b, c, d, e, f, g). EHT analysis suggests that the X-ray luminosity is $\langle L_{\rm X} 10^{-2\sigma} \rangle < 4.4 \times 10^{40}$ erg s^{-1} and the jet power is $P_{\rm jet} > 10^{42}$ erg s^{-1}. The radiative efficiency is smaller than the corresponding thin disc efficiency (EHT Collaboration 2019f).

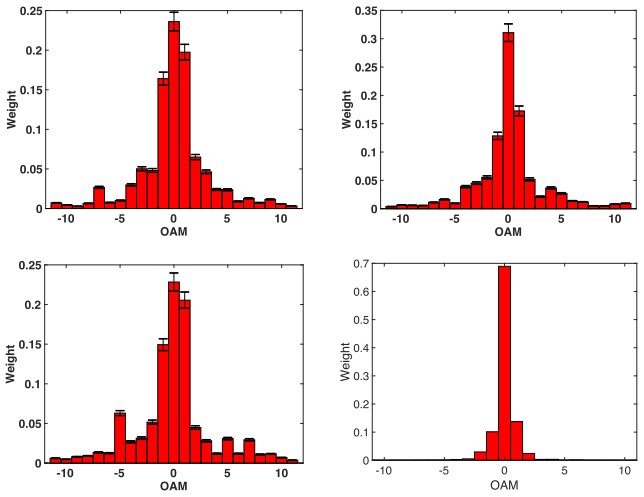

Figure 2. OAM spectra from the results of SMILI, EHT (up), and DIFMAP (bottom left) data analyses by EHT of the observation taken on 2017 April 11 (EHT Collaboration 2019a, e, g) and from the numerical simulations with KERTAP. The data considered here represent the visibility amplitude and phase, provided by EHT, as a function of the vector baseline. As the spatial phase distribution is, in this case, present in the data, we do not need to apply the TIE method to recover it. In all the data sets, the asymmetry parameter, the ratio q between the $m = 1$ and -1 peaks in the spiral spectra, is $q > 1$, indicating a clockwise rotation with $i = 17^\circ$ if the angular momentum of the accretion flow and that of the black hole are anti-aligned (equivalent to a similar geometry with $i = 163^\circ$, where angular momentum of the accretion flow and that of the BH are aligned). Bottom right: The value of q, obtained from the spiral spectrum of KERTAP simulations, has an error of $\sim 10^{-7}$, in agreement with the values found from these results and the TIE method.

Our results above, obtained using the TIE methodology, show good agreement with those resulting from a more constraining approach, i.e. that which directly utilizes the visibility amplitude and the phase maps for the day 2017 April 11 released by EHT. In particular, the ETH collaboration applied three data analysis methods: DIFMAP, EHT, and SMILI, (EHT Collaboration 2019a, e, g). We obtained $q_{\rm DIFMAP} = 1.401 \pm 0.047$, $q_{\rm EHT} = 1.361 \pm 0.046$, and $q_{\rm SMILI} = 1.319 \pm 0.045$, yielding for this day an averaged value of $\overline{q} = 1.360 \pm 0.027$ ($a = 0.821 \pm 0.062$). This value deviates by a quantity $\Delta a \simeq 0.087$ from that of epoch 2 obtained with the TIE method. Since, in all cases, it results $q > 1$, the clockwise sense of rotation is confirmed. The spiral spectra of this additional data analysis are reported in Fig. 2.

The error in the final estimate of a depends on the numerical error of the TIE reconstruction method, $|\Delta a|_{\rm TIE} \sim 10^{-7}$, and from that of the final EHT data products that include the calibrated total intensity amplitude and phase information. The latter are validated through a series of quality-assurance tests and show consistency across

pipelines setting limits on baseline systematic errors of 2 per cent in amplitude and 1° in phase, giving a maximum error chi-squared test of ∼ 5 per cent (EHT Collaboration 2019b, c, d, e). By averaging for any point in the image, the values in a neighbourhood of three pixels, we reduce the error in the calculation of the OAM spectrum, $|\Delta a|_{\rm EHT} \simeq 0.046$. This ensures a good precision in the reconstruction of the surroundings of the BH and for our OAM analysis. The total error of a becomes

$$|\Delta a|_{\rm tot} = |\Delta a|_{\rm TIE} + |\Delta a|_{\rm EHT} \simeq 0.046\,, \qquad (2)$$

hence yielding a first conservative estimate of the rotation parameter at $a = 0.904 \pm 0.046$, with an ∼ 95 per cent confidence level (c.l.), and the hypothesis of a static BH is excluded at $\sim 6\sigma$. More details can be found in the SM.

Even if the spatial phase profile was not measured directly for the values of q obtained with the TIE method, something that can be achieved with interferometric or other more direct techniques, the values of the rotation parameter a obtained with the OAM method agree with the experimental data obtained from results presented in the literature. Preferably, one should take a succession of snapshots with the EHT at much shorter time intervals, typically a few minutes rather than days, to improve the accuracy of the terms in the TIE of equation (6) in the SM. This could be realized quite straightforwardly.

With dedicated observations and new fiducial pipeline images of amplitude and phase plots, and new interferometric methods that analyse the EM field in intensity and phase (readily realized with standard radio telescopes as was reported for the fiducial pipeline images of the visibility amplitude and phase plots for 2017 April 11), one should be able to drastically improve the measurements of the OAM content within the spiral spectrum of the EM radiation emitted in the neighbourhood of rotating black holes. As second step, it will be possible to estimate in a more accurate way the BH rotation and the other fundamental parameters of the system from the shape of the shadow. Ultimately, radio telescopes equipped with antenna systems optimized to directly capture and resolve the EM angular momentum in the signals received should be able to unleash the full potential of the OAM in observational astronomy. One advantage of involving OAM in black hole astronomy is that polarization and OAM together build up the total angular momentum invariant $\boldsymbol{J}$, and when polarization is affected by the presence of polarizing media such as dust and unstructured plasma, OAM will be less affected and can be used as a reference point to extract additional information about the source from its emitted light.

3 CONCLUSIONS

Exploiting the properties of the Kerr metric, we were able to measure the rotation of M87* by analysing a sequence of images acquired by the EHT. In particular, the estimate of the rotation parameter a was derived from the characterization of the vorticity of the EM waves emitted from the surroundings of the BH, affected by a strong gravitational lensing from the rotating compact object (Tamburini et al. 2011a). The OAM and the EM vorticity were reconstructed from the public released images of the brightness temperature of the Einstein ring of the M87 black hole, taken during four different days with a well-known technique based on the TIE (Rybicki & Lightman 2004; Lubk et al. 2013; Zhang et al. 2015) that permits the reconstruction of the phase wavefront and of the OAM content from two or more consecutive acquisitions of the same source taken at different distances.

By applying the general relativistic effect in the Kerr metric discussed in Tamburini et al. (2011a), we find that the central black hole in M87 is rapidly rotating clockwise with rotation parameter $a = 0.90 \pm 0.10$ and inclination $i = 17^\circ \pm 2^\circ$ (equivalent to a magnetic arrested disc with an inclination $i = 163^\circ \pm 2^\circ$) with a 95 per cent c.l., and the case for a non-rotating BH is excluded with an $\sim 6\sigma$ c.l. This enormous amount of energy trapped in the black hole rotation implies a rotational energy of about 10^{64} erg, comparable to the energy emitted by the brightest quasars over Gyr time-scales (Christodoulou & Ruffini 1971).

ACKNOWLEDGEMENTS

We thank Guido Chincarini for help and useful discussions. FT acknowledges ZKM and Peter Weibel for the financial support. The encouragement and support from Erik B. Karlsson is gratefully acknowledged.

REFERENCES

Anderson T. W., 1994, Statistical Analysis of Time Series. John Wiley and Sons, New York, NY, USA
Anzolin G., Tamburini F., Bianchini A., Umbriaco G., Barbieri C., 2008, A&A, 488, 1159
Bambi C., Freese K., Vagnozzi S., Visinelli L., 2019, Phys. Rev. D, 100, 044057
Barbero S., 2006, Opt. Express, 45, 094001
Barnett S. M., Allen L., 1994, Opt. Commun., 110, 670
Beckwith K., Done C., 2005, MNRAS, 359, 1217
Carini P., Geng L.-L., Li M., Ruffini R., 1992, Phys. Rev. D, 46, 5407
Chen B., Kantowski R., Dai X., Baron E., Maddumage P., 2015, ApJS, 218, 4
Christodoulou D., Ruffini R., 1971, Phys. Rev. D, 4, 3552
Dehnen H., 1973, Int. J. Theor. Phys., 7, 467
De Zela F., 2012, in Pahlavani M. R., ed., Theoretical Concepts of Quantum Mechanics, Chapt. 14. IntechOpen, Weinheim, DE, p. 289
Doeleman S. S. et al., 2012, Science, 338, 355
Doi A., Hada K., Nagai H., Kino M., Honma M., Akiyama K., Oyama T., Kono Y., 2013, in Gómez J. L., ed., EPJ Web Conf. Vol. 61, ALMA Continuum Spectrum of the M87 Nucleus. EDP Sci., Les Ulis Cedex A, France, p. 08008
EHT Collaboration, 2019a, EHT Data Products, Online Image Data. https://eventhorizontelescope.org/for-astronomers/data
EHT Collaboration, 2019b, ApJ, 875, L1
EHT Collaboration, 2019c, ApJ, 875, L2
EHT Collaboration, 2019d, ApJ, 875, L3
EHT Collaboration, 2019e, ApJ, 875, L4
EHT Collaboration, 2019f, ApJ, 875, L5
EHT Collaboration, 2019g, ApJ, 875, L6
Feng L.-L., Lee W., 2001, Int. J. Mod. Phys. D., 10, 961
Harwit M., 2003, ApJ, 597, 1266
Kelly D. P., 2018, Int. J. Opt., 2018, 1
Kerr R. P., 1963, Phys. Rev. Lett., 11, 237
Lubk A., Guzzinati G., Börrnert F., Verbeeck J., 2013, Phys. Rev. Lett., 111, 173902
Molina-Terriza G., Torres J. P., Torner L., 2007, Nat. Phys., 3, 305
Ruelas A., Lopez-Aguayo S., Gutiérrez-Vega J. C., 2018, J. Opt., 21, 015602
Rybicki G. B., Lightman A. P., 2004, Radiative Processes in Astrophysics. Phys. Textbook, Wiley, Weinheim
Schulze C., Naidoo D., Flamm D., Schmidt O. A., Forbes A., Duparré M., 2012, Opt. Express, 20, 19714
Sob'yanin D. N., 2018, MNRAS, 479, L65
Su F. S., Mallett R. L., 1980, ApJ, 238, 1111
Tamburini F., Thidé B., Molina-Terriza G., Anzolin G., 2011a, Nat. Phys., 7, 195

Tamburini F., Mari E., Thidé B., Barbieri C., Romanato F., 2011b, Appl. Phys. Lett., 99, 204102
Tamburini F., Mari E., Sponselli A., Thidé B., Bianchini A., Romanato F., 2012, New J. Phys., 14, 03301
Thidé B. et al., 2007, Phys. Rev. Lett., 99, 087701
Thidé B., Elias N. M., II, Tamburini F., Mohammadi S. M., Mendonça J. T., 2011, in Torres J. P., Torner L., eds, Twisted Photons: Applications of Light With Orbital Angular Momentum, Chapt. 9. Wiley-VCH Verlag, John Wiley and Sons, Weinheim, DE, p. 155
Torner L., Torres J. P., Carrasco S., 2005, Opt. Express, 13, 873
Torres J. P., Torner L., 2011, Twisted Photons: Applications of Light With Orbital Angular Momentum. Wiley-VCH Verlag, John Wiley and Sons, Weinheim, DE
Wold H., 1954, A Study in the Analysis of Stationary Time Series, 2nd edn. Almqvist and Wiksell, Uppsala, Sweden
Yang H., Casals M., 2014, Phys. Rev. D, 90, 023014
Zhang D., Feng X., Cui K., Liu F., Huang Y., 2015, Sci. Rep., 5, 11982

SUPPORTING INFORMATION

Supplementary data are available at *MNRASL* online.

SIM_final_rev3.pdf

Please note: Oxford University Press is not responsible for the content or functionality of any supporting materials supplied by the authors. Any queries (other than missing material) should be directed to the corresponding author for the article.

This paper has been typeset from a TEX/LATEX file prepared by the author.